EUROPEAN ORGANIZATION FOR NUCLEAR RESEARCH S82

PH I/COM-38/68
24 June, 1968

PHYSICS I

ELECTRONICS EXPERIMENTS COMMITTEE

PROPOSAL

FOR AN ACCURATE DETERMINATION OF THE RATIO η_{oo}/η_{+-}

by

V. Bisi, P. Darriulat, H. Faissner, M.I. Ferrero,
H. Karl, C. Grosso, K. Kleinknecht, C. Rubbia,
A. Staude and K. Tittel

CERN-Aachen-Torino
Collaboration

EUROPEAN ORGANIZATION FOR NUCLEAR RESEARCH

PROPOSAL FOR AN ACCURATE DETERMINATION OF THE RATIO η_{00}/η_{+-}

V. Bisi, P. Darriulat, H. Faissner, M.I. Ferrero, H. Karl, C. Grosso, K. Kleinknecht, C. Rubbia, A. Staude, and K. Tittel.

CERN-Aachen-Torino
Collaboration

ABSTRACT: A proposal is presented which is intended to measure the ratio $\left|\frac{\eta_{00}}{\eta_{+-}}\right|$ to an accuracy of about $\pm 3.0\%$. Decay modes $K_{S,L} \rightarrow \pi^+\pi^-$ are detected by the magnetic spectrometer and wire chambers built for our recent K_L-K_S mass difference determination (S49). Decay modes $K_{S,L} \rightarrow \pi^0\pi^0$ are detected by wire chambers and Total Absorption Gamma-ray Hodoscope. The measurements are to be carried out in such a way that the result is independent of the geometrical and momentum acceptances of the detectors.

Geneva - June 1968

1. INTRODUCTION

In a recent paper, J.M. Gaillard et al(1) have reported a measurement of the decay rate $K_L \rightarrow \pi^0 \pi^0$. The measurement of a neutral decay rate is of fundamental importance in the understanding of the phenomenology of CP violation in K_0 decays. We define as usual:

$$\eta_{+-} = \frac{A(K_L \rightarrow \pi^+ \pi^-)}{A(K_S \rightarrow \pi^+ \pi^-)} = (\varepsilon + \varepsilon') \qquad [1.1]$$

$$\eta_{00} = \frac{A(K_L \rightarrow \pi^0 \pi^0)}{A(K_S \rightarrow \pi^0 \pi^0)} = \varepsilon - 2\varepsilon' \qquad [1.2]$$

where ε is a measure of the CP violation in the $K_0 - \bar{K}_0$ mass matrix and ε' is related to CP violations in the decay channel arising from interferences between final states of different isospin. The arguments of the complex quantities ε and ε' are in principle known from CPT Invariance and Conservation of Probability:

$$\arg(\varepsilon') = \delta_0 - \delta_2 - \pi/2$$

$$\arg(\varepsilon) = \arctan \frac{2(m_S - m_L)}{\Gamma_S - \Gamma_L} + \varphi_R$$

where φ_R is related to the CP violation in decay channels other than the two pion modes and δ_0, δ_2 are the (π, π) scattering phase shifts in the T = 0, T = 2 states, Γ_S, m_S, Γ_L, m_L are lifetimes and masses of the short-lived and long-lived states. If $\varphi_R \approx 0$, $\arg(\varepsilon) = 43^\circ \pm 1.5^\circ$, and according to Walker(4), $\delta_0 - \delta_2 = 50^\circ \pm 20^\circ$.

The "superweak" model of Wolfenstein(5) predicts $\varepsilon' = 0$ and therefore, $\eta_{+-} = \eta_{oo}$. Defining:

$$\Omega_{oo} = \frac{\text{Rate } (K_L \to \pi^\circ \pi^\circ)}{\text{Rate } (K_S \to \pi^\circ \pi^\circ)}$$

$$\Omega_{+-} = \frac{\text{Rate } (K_L \to \pi^+ \pi^-)}{\text{Rate } (K_S \to \pi^- \pi^+)}$$

for $|\varepsilon'| << |\varepsilon|$, expressions [1.1] and [1.2] can be expanded as follows:

$$\frac{\Omega_{oo}}{\Omega_{+-}} = \frac{|\eta_{oo}|^2}{|\eta_{+-}|^2} = 1 + 6\left|\frac{\varepsilon'}{\varepsilon}\right| \cos\left(\delta_o - \delta_2 - (43^\circ \pm 1^\circ)\right) + \text{ terms order } \left|\left(\frac{\varepsilon'}{\varepsilon}\right)\right|^2$$

$$\simeq 1 + 6\left|\frac{\varepsilon'}{\varepsilon}\right| \cos(9^\circ \pm 20^\circ) + \ldots$$

The present proposal is dealing with an experiment to measure directly the ratio $\frac{\Omega_{oo}}{\Omega_{+-}}$ to an accuracy of about 6%. Therefore the ultimate sensitivity to (small) deviations from the "superweak" model is expected to be $\left|\frac{\varepsilon'}{\varepsilon}\right| \simeq 10^{-2}$.

2. PRINCIPLE OF THE EXPERIMENT

The measurement is a relative one and it is based on a comparison between decay modes $K_L \to \pi^+\pi^-$ and $K_L \to \pi^\circ\pi^\circ$ in experimental conditions as identical as possible. Decay rates are normalized to the corresponding short-lived decay modes $K_S \to \pi^+\pi^-$ and $K_S \to \pi^\circ\pi^\circ$ after a thick copper regenerator. Source distributions of the short-lived and long-lived decays are made closely identical by continuously moving the regenerator along the decay volume. The momentum spectra for both decay modes are also made practically equal by a specific choice of the geometry of the regenerator. Thus the measurement is made to a high degree independent of the actual geometrical detection efficiencies and of the knowledge of the momentum spectrum.

Identity of distributions in all measurable physical quantities related to the two pion mode between the short-lived and long-lived runs is a powerful test of the correct performance of the detector. Furthermore, experimental distributions can be accurately predicted with Monte Carlo calculations.

We intend to detect the charged mode with our present wire chamber spectrometer. The apparatus is very well understood and it has provided so far several millions of K_o decays. The events are reconstructed by measuring vector momenta of both charged prongs . The invariant mass of the charged pair is measured to about ± 6 MeV and the direction of the resultant momentum to about $\pm 3 \times 10^{-3}$ radiants. It has been normally possible to collect about 2000 $K_L \rightarrow \pi^+ \pi^-$ events/day in good background conditions. The transmission regenerated event rate of a thick regenerator was about one order of magnitude larger.

The magnetic spectrometer will be then removed and replaced with a total absorption γ-spectrometer looking at the same decay region and designed to fit to the present data acquisition system and on-line computer.

Following the principle already experienced by Gaillard et al$^{(1)}$, Fitch et al$^{(2)}$, S. Parker et al$^{(3)}$, all four gamma-rays are required to convert in spark chambers. However, important differences must be noted:

i) Absolute gamma-ray energies are measured by a Lead Glass Hodoscope made of 25 separate elements, rather than energy ratios by visual spark counting. The accuracy of the lead glass counter is about a factor 2.5 better and, most important fact, free of "difficult" cases in which abnormal shower development requires subjective judgement criteria.

ii) Gamma-ray directions are determined by looking at the electron-positron pair generated in a thin (0.5 mm) lead plate rather than from the early part of the shower development. The expected accuracy in the square of the angle of the reconstructed K_o direction is about a factor 10 better than in Ref. (1).

iii) The events rate is high because of the small production angle (7^o) of the neutral beam and the liberal trigger condition permitted by the short dead time (~ 3 ms) of the wire chambers. It is expected that the final sample would consist in a few thousand of $K_L \rightarrow \pi^o \pi^o$ events in clean background conditions.

Angle and energy resolutions are sufficient to reconstruct the invariant mass of the two γ-ray pairs accurately enough to remove pairing ambiguities. The $K_L \rightarrow \pi^o \pi^o \pi^o$ background is expected to be negligible.

3. DETECTION OF THE FOUR GAMMA RAYS

The average K_o energy is 4.0 GeV/c. Therefore the average photon energy is expected to be of the order of 1.0 GeV/c. We require a good knowledge of the energies of all four γ-rays. The decay angles are obtained best as already remarked by J.M. Gaillard et al(1) from a fit to the point of decay. Therefore it is sufficient in principle to know accurately two gamma rays directions and the remaining two only to the extent required to eliminate accidental solutions. However, to have a valid constraint in the fit we shall ask to determine three out of four gamma directions accurately and a more modest precision for the remaining fourth photon. The gamma detector (see Figs. 1 and 2) can be visualized in three separate parts:

i) a "long" conversion length region made out of several thin lead sheets and subsequent wire chamber planes in which direction of three gamma-rays out of four are determined;

ii) a "short" conversion length region made out of thicker lead plates for the fourth γ-rays conversion;

iii) a Total Absorption γ-ray Hodoscope in which most of the energy of the gamma rays is dissipated. The four γ-rays are required to trigger distinct elements of the hodoscope. As discussed below, the γ-ray hodoscope could be made either out of lead glass blocks (Fig. 1) or lead-scintillator sandwiches (Fig. 2). Two schemes are quite similar and the final choice can be made only after careful comparison of performance of the two prototypes.

The accuracy in spark position determination for our present wire chambers (S49) has been determined to be $\sigma = 0.35$ mm. For the chosen spacing between chambers, the precision in the γ-ray direction is mostly determined by Coulomb scattering in the radiator. The thickness of the lead converters in front of the chambers is determined as a compromise between accuracy and detection efficiency. The detection efficiency versus the total number of conversion lengths of the wire chambers is given in Fig. 3. We have chosen 5 chambers $\frac{1}{10}$ conversion lengths thick corresponding to a total of 0.5 conversion lengths that is to an average conversion length about 10 times ~~smaller~~ longer than the one of Ref. (1). We shall assume in the angular measurement of a 500 MeV/c incident photon a precision equal to $\sqrt{10}$ times the one observed by J.M. Gaillard et al$^{(1)}$. Since Coulomb scattering is expected to be the main source of uncertainties the precision has been extrapolated according to a $\frac{1}{E_\gamma}$ law.

The "short" conversion length region is made out of lead plates $\frac{1}{4}$ conversion lengths thick followed by wire chambers. In order to remove ambiguities in reconstruction two of the four sets of chambers (u, v) have wires oriented at 45° from the orthogonal wire planes directions (X, Y) of the remaining chambers. The accuracy in the angular direction of the fourth γ-ray converting in these chambers is assumed to be much poorer . The primary task of this second set of chambers is a determination of the conversion point of the fourth γ-ray.

Secondary radiative effects after conversion in a 1/10 radiation-length thick converter are negligible. At the exit of the plate 5% of the incident energy is on the average carried by photons. Early conversion of these γ-rays into electrons or e^+e^- paris is very unlikely. From extrapolation of showers calculations of Messel et al (4), we estimate to less than 1% the probability of observing a second electron conversion ($E_e > 10$ MeV). The general apparence of the conversion of electron pair in the two first pairs of wire chamber planes is a single spark. The detection efficiency for a single track is presently $\geq$ 97%. Therefore the detection efficiency for two particles is expected to be $\geq$ 99.9% and no duplication of the wire planes is foreseen. However, chamber wires are cut in the middle and separated electrically. Read-out is done at both (opposite) sides. In this way, each pair of chamber planes with orthogonal wires is effectively divided in four independent quadrants. A small insensitive region is introduced at the center of each chamber to reduce beam associated backgrounds.

Figure 4 is a summary of the status of the Art of building gamma detectors, taken from the paper of D. Luckey at the Hamburg Conference in 1965. Visual track counts refer to counting of sparks or tracks in the gap of a multiple spark chamber. All resolutions are measured under ideal conditions with mono-energetic electrons. Precise knowledge of the point of impact of the shower on the counter is provided in our case by the wire chambers: therefore we expect to be not too far from this "idealized" case.

Two types of detector appear competitive. They are:

i) total absorption Cerenkov counter, and

ii) lead scintillator sandwich.

The Cerenkov counter hodoscope could be made out of some 25 elements. Each counter of the hodoscope is a rectangular parallelepiped of Schott SF5 flint glass with dimension 30 x 30 x 35 cm^3 viewed from the back and by several (3?) cheap 5" photomultiplier (54AVP). This is a commonly made optical glass which has a radiation length of 3.0 cm. Each block is separated optically. Pulse heights in individual counters are separately recorded. The gain of individual counters could be set equal, for instance with a weak source imbedded in small NaI cristals or alternatively light-pulsers. The lead-scintillator sandwich is shown in Figure 5. Only one 5" phototube is adequate for optimum light collection. Figure 6 shows how 20 counters could be stacked to form the hodoscope. The lead-scintillator sandwich is probably of easier construction, but it has somewhat poorer energy resolution.

We intend to optimize all parameters of the γ-ray detector by preliminary investigations with an electron beam. The choice between the lead scintillator and Cerenkov hodoscope will be taken at this later stage.

4. DETECTION OF $K_{L,S} \to \pi^0 \pi^0$ EVENTS

The experimental arrangement is shown in Figure 1 (lead scintillator sandwich) and Figure 2 (Cerenkov counter). Neutral decay events occuring over a 2.5 m long decay path are recorded. The trigger condtions are as follows:

i) at least 2 vertical and 2 horizontal elements of the 10 X, 10 Y Hodoscope Counter Array;

ii) a total energy dissipated in the absorption gamma counters larger than 2.0 GeV/c;

iii) at least 3 or 4 cells of the Total Absorption Hodoscope above an energy threshold of some 100 MeV;

iv) no anticoincidence count and no guard anticoincidence count;

v) eventually no count in the veto funnel.

Considering the large size of this counter, it might be advisable however to segment this counter and to record the information on tape only. The central region of the total absorption hodoscope is blanked out and a recessed gamma ray anticoincidence counter is located in the neutral beam line.

The geometrical detection efficiency for the decay process $K_L \to \pi^0 \pi^0$ is shown in Figure 6. A lower energy threshold of 200 MeV has been required for each of the four gamma rays. The detection efficiency is higher in the case of the lead scintillator sandwich because the segmentation of the hodoscope surface is better. For comparison, the detection efficiency of the magnetic spectrometer and wire chambers to be used for the charged decay mode $K_L \to \pi^+ \pi^-$ is also shown. In the region of interest (kaon momentum $\geqslant 3$ GeV/c), the energy dependence of the detection efficiencies for the charged and the neutral modes are remarkably similar.

Decay events of the type $K_S \rightarrow \pi^0\pi^0$ are generated by placing a 20 cm thick copper regenerator in the neutral beam. The choice of the size and the material is based on the following points:

i) The amount of regeneration obtained is large. We have recently measured immediately after the regenerator a decay rate for charged two pions mode about 1000 times the CP violating $K_L \rightarrow \pi^+\pi^-$ decay rate. Therefore corrections due to interference effects between K_L and K_S decay amplitudes are small.

ii) The ratio R between diffraction regeneration and transmission regeneration in the forward cone is small. Taking

$$p_K = 4.0 \text{ GeV/c} \qquad \Delta\Omega = 5 \times 10^{-5}$$

we get $R = 1/70$.

iii) The regeneration amplitude is found to be independent of energy in the interval 2.75 to 7.0 GeV/c (Figure 7). This is so because for the regenerator thickness "ad hoc" chosen, the increasing regeneration cross section at lower energies is almost exactly compensated by a decrease of the geometrical factor coming from the shorter decay path and mass difference oscillations.

iv) Changed decay events $K_S \rightarrow \pi^+\pi^-$ taking place inside the regenerator are eliminated by an anticoincidence counter. Neutral decays in which none of the four γ-rays converts in the regenerator material are normally counted. The short radiation length in copper makes this correction very small ($\sim$1.8%).

The source distribution of K_S decay events is made uniform by moving the regenerator block back and forth along a volume larger than the decay region at a speed proportional to the neutral beam intensity. The basic idea behind is as follows: adding a large number of decay distributions of <u>any</u> shape vanishing(*) at $+\infty$ and $-\infty$ [of equal weights per unit of deplacement] generates a flat distribution. Thus the measurement is made independent of the knowledge of the detection efficiency.

Measurements with and without regenerator should alternate as often as possible to average over possible detector and monitoring drifts. The measured ratio of two pi-zero events per unit of neutron monitor counts R_{00} gives:

$$R_{00} = \text{const} \times |\rho|^2 \times \Omega_{00}$$

where ρ is the regeneration amplitude, and the constant depends exclusively on the length over which the regenerator slab is moved.

A similar expression is valid for the charged decay mode exposure:

$$R_{+-} = \text{const} \times |\rho|^2 \times \Omega_{+-}$$

and the value of the constant is the same provided the same regenerator moving mechanism is used. It is important to

---

(*)We neglect $K_L \to \pi^0\pi^0$ respect to $K_S \to \pi^0\pi^0$ or rather we shall introduce a small ($\sim$ 1.0%) correction for this effect.

stress that expressions do not contain the kaon momentum because the regeneration amplitude is made deliberately momentum independent. Also the monitoring constants could be different for charged and neutral decay measurements.

Combining formulae [4.1] and [4.2], we get that the final result is given by:

$$\left|\frac{\eta_{00}}{\eta_{+-}}\right|^2 = \frac{\Omega_{00}}{\Omega_{+-}} = \frac{R_{00}}{R_{+-}}$$

5. DATA ANALYSIS

In order to simulate the analysis procedure a Monte Carlo calculation was performed in which $K \rightarrow \pi^\circ \pi^\circ$ events were generated. Events are required to satisfy to the trigger criteria and to the condition $E_\gamma > 200$ MeV. In order to take into account measurement~~s~~ errors, γ-rays angles and energies have been smeared according the assumed standard deviations. The main conclusions of the calculation are as follows:

1) The π_0 mass can be reconstructed with an error $\sigma_{\pi_0} =$ 20 MeV. (standard dev.). Only $\sim 0.1\%$ of the two other wrong γ-ray pairings gives apparent π_0's masses within 2.5 standard deviations from the true value. Therefore measurement of the two 2γ's invariant masses is adequate to resolve ambiguities due to alternate pairings.

2) The visible energy and the reconstructed 2 γ's energy under the assumption of $\pi^o \rightarrow 2\gamma$ decay of the 2 's is determined to about $\sigma = 130$ MeV (for the correct γ's pairings).

3) The four γ's invariant mass is determined to about $\sigma_{4\gamma} = 63$ MeV. The K_o invariant mass for a fitted decay vertex is determined to about $\sigma_{\pi^o\pi^o} = 6.0$ MeV, that is: the accuracy is equal to the one in the charged mode.

4) The reconstructed K_o direction is measured to an accuracy in the square of the K_o ~~direction~~ angle of about 2×10^{-5}, which is about two times worse than for the charged mode.

In order to evaluate the background events produced by $K_o \rightarrow \pi^o\pi^o\pi^o$ events in which 2 γ's escape detection, a similar Monte Carlo calculation was performed for the 3 π^o decays in which it has been assumed (somehow arbitrarily) that all γ-rays below 100 MeV are escaping detection and above 100 MeV they are detected with 90 % efficiency. Events are selected with the following criteria:

i) reconstructed K_o direction $\theta_K^2 \leq 6 \times 10^{-5}$;

ii) reconstructed 2 γ masses within 2.5 standard deviations from the π^o mass;

iii) visible energy and computed energies for $\pi^o \rightarrow 2\gamma$ decay of each γ-pair compatible within 2.5 standard deviations.

All possible γ-ray pairing are tried out. The calculation indicates (Figure 8) a negligible background from $K \rightarrow \pi^o\pi^o\pi^o$ events.

6. CONCLUDING REMARKS

Let us assume that the result of J.M. Gaillard et al$^{(1)}$ is to be confirmed by the presently proposed measurement. Then: Rate($K_L \rightarrow \pi^+\pi^-$) $\cong$ Rate($K_L \rightarrow \pi^0\pi^0$). Geometrical detection efficiencies for the $K_L \rightarrow \pi^+\pi^-$ and $K_L \rightarrow \pi^0\pi^0$ modes are about equal. The over-all conversion probability for the four γ-rays is about 0.1. Therefore the good events rate for the measurement of the neutral decay mode is expected to be about 1/10 of the charged one, that is about 200 events/day.

The measurement of the rate $K_L \rightarrow \pi^0\pi^0$ is evidently the most time-consuming one. Let us assume to run 15 full days, corresponding to 3000 good events. The statistical error is then $1/\sqrt{3000} = 1.8\%$. Assuming arbitrarily that background substraction and measurements of $K_L \rightarrow \pi^+\pi^-$ $K_S \rightarrow \pi^+\pi^-$, $K_S \rightarrow \pi^0\pi^0$ rates for which statistical errors are negligible increase the measurement error by π, we get the ratio $\left|\frac{\eta_{00}}{\eta_{+-}}\right|$ to about ± 6%.

FIGURE CAPTIONS

Fig. 1 :	Detector for $K_{L,S} \rightarrow \pi^o\pi^o$ decay. The decay region is surrounded by veto counters. A region with long conversion length and 5 wire chamber planes is followed by a region with short conversion length and a lead sandwich total absorption counter.
Fig. 2 :	Same detector as in Fig. 1, but with lead glass total absorption counters.
Fig. 3 :	Conversion probabilities for 2, 3 or 4 γ's converting as a function of the convertor thickness.
Fig. 4 :	Resolution of different types of γ - detectors. From D. Luckey, Hamburg Symposium on Photon Interactions.
Fig. 5 :	Arrangement of lead scintillator sandwich counters.
Fig. 6 :	Geometrical efficiencies for detection of $K_o \rightarrow \pi^o\pi^o$ decays for the detectors in Figs. 1 and 2, resp. Efficiencies for detecting $K_o \rightarrow \pi^+\pi^-$ in the existing wire chamber spectrometer are also shown.
Fig. 7 :	Regeneration amplitude ρ behind a 20 cm Copper Regenerator for different K_L momenta (measured by the group).

Fig. 8 : Background events from $K_L \rightarrow \pi^0\pi^0\pi^0$ decays in which 2 γ-ray escape detection. The invariant mass distribution shown in for $K_o \rightarrow \pi^0\pi^0$ decays is much wider than the value indicated in the text because the constraint on decay point has not been used in the γ-ray direction determinations.

REFERENCES

(1) J.M. Gaillard, W. Galbraith, A. Hussri, M.R. Jane, N.H. Lipman, G. Manning, and T.J. Ratcliffe, H. Faissner and H. Reithler, RPH/H/35 (1968), to be published.

(2) T. Kamae, Bull. Am. Phys. Soc., 13, 31 (1968), and V.L. Fitch, Private communication.

(3) S. Parker, Bull. Am. Phys. Soc., 13, 31 (1968), and V.Z. Peterson, Private communication.

(4) H. Messel, A.D. Smirmow, A.A. Vartelomeev, D.F. Crawford and J.C. Butchner, Nucl. Phys. 38, 1, (1962).

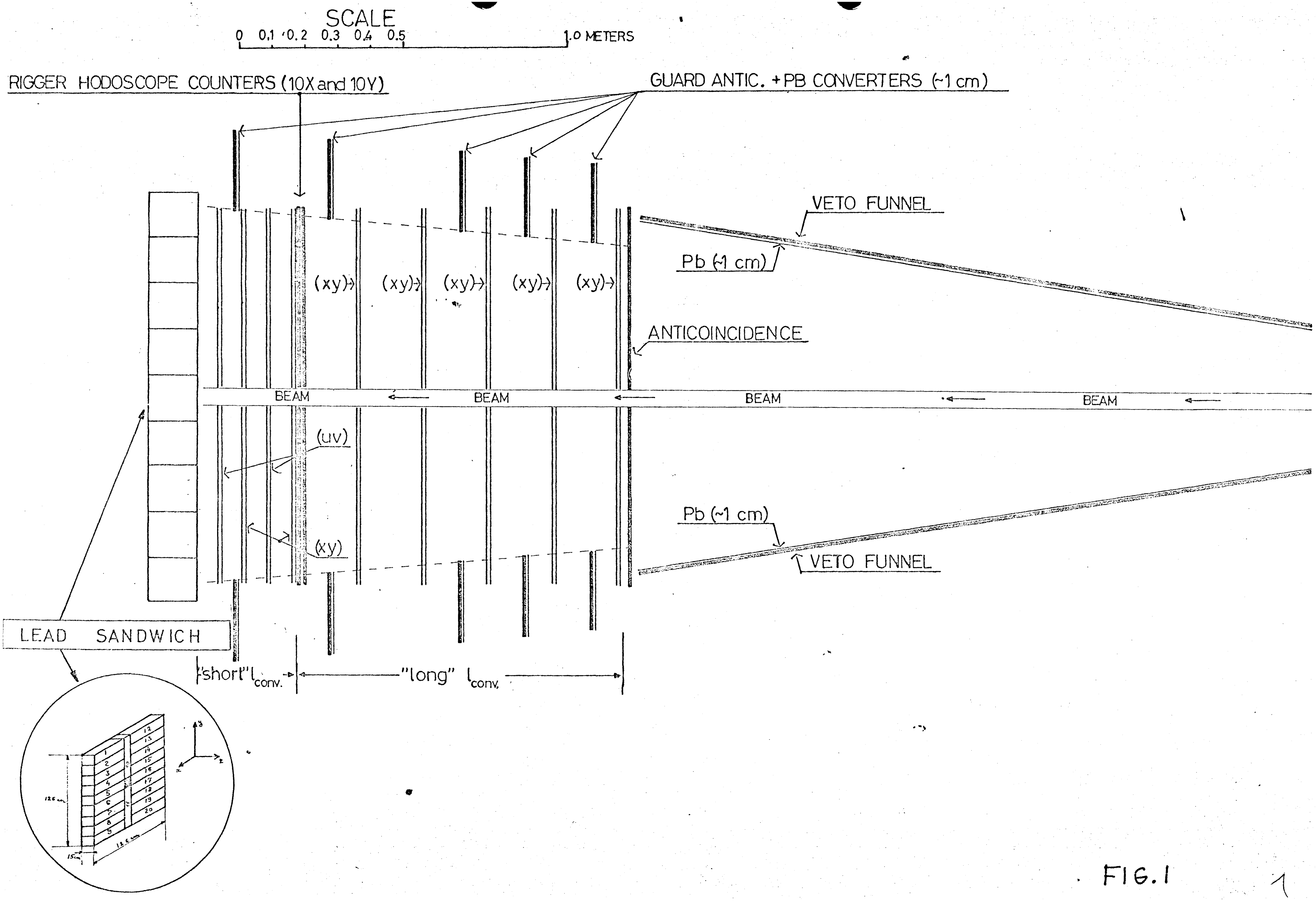
SCALE
0 0.1 0.2 0.3 0.4 0.5 1.0 METERS
RIGGER HODOSCOPE COUNTERS (10X and 10Y)
GUARD ANTIC. + PB CONVERTERS (~1 cm)
VETO FUNNEL
Pb (~1 cm)
(xy)
(xy)
(xy)
(xy)
(xy)
ANTICOINCIDENCE
BEAM
BEAM
BEAM
BEAM
(uv)
(xy)
Pb (~1 cm)
VETO FUNNEL
LEAD SANDWICH
"short" l conv.
"long" l conv.
126 cm
15 cm
12.6 cm

FIG.1

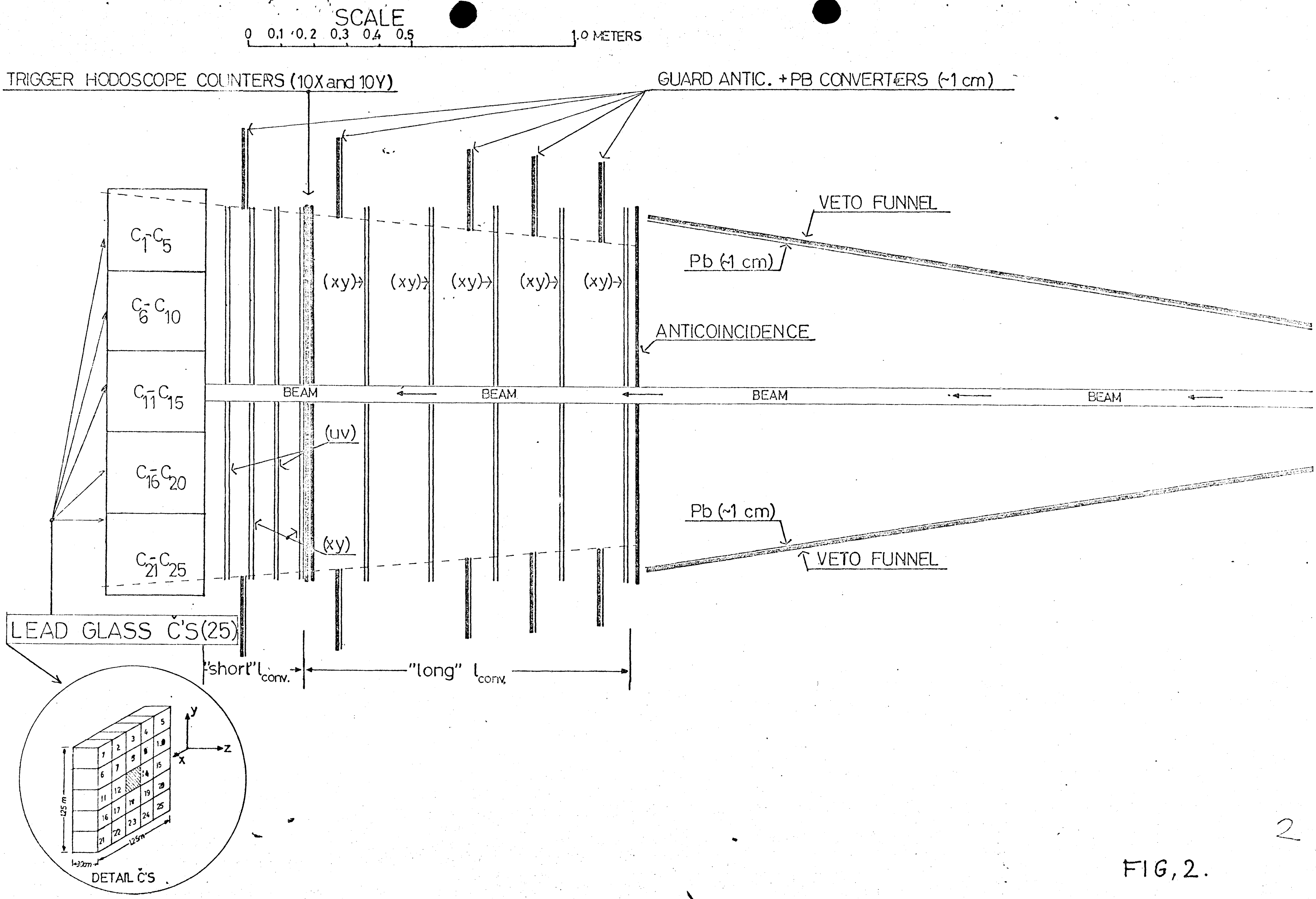
SCALE
0 0.1 0.2 0.3 0.4 0.5 1.0 METERS
TRIGGER HODOSCOPE COUNTERS (10X and 10Y)
GUARD ANTIC. + PB CONVERTERS (~1 cm)
VETO FUNNEL
Pb (~1 cm)
ANTICOINCIDENCE
(xy)
(xy)
(xy)
(xy)
(xy)
BEAM
BEAM
BEAM
BEAM
(uv)
(xy)
Pb (~1 cm)
VETO FUNNEL
C1-C5
C6-C10
C11-C15
C16-C20
C21-C25
LEAD GLASS Č'S (25)
"short" lconv.
"long" lconv.
y
z
x
1.25 m
1.25 m
.30 m
DETAIL Č'S

FIG, 2.

2

FIG. 3.

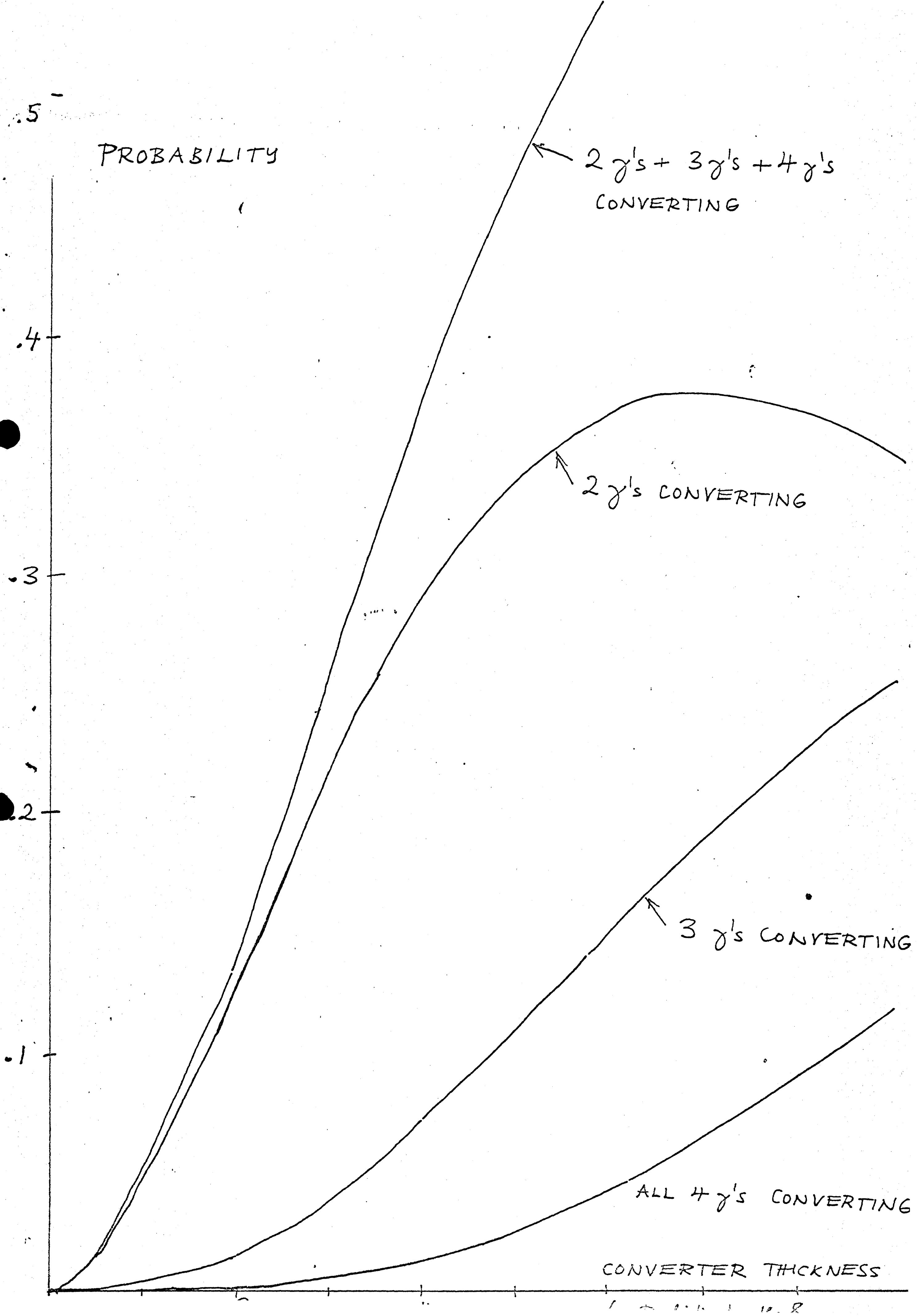

.5
PROBABILITY
.4
.3
.2
.1
2 γ's + 3 γ's + 4 γ's CONVERTING
2 γ's CONVERTING
3 γ's CONVERTING
ALL 4 γ's CONVERTING
CONVERTER THICKNESS

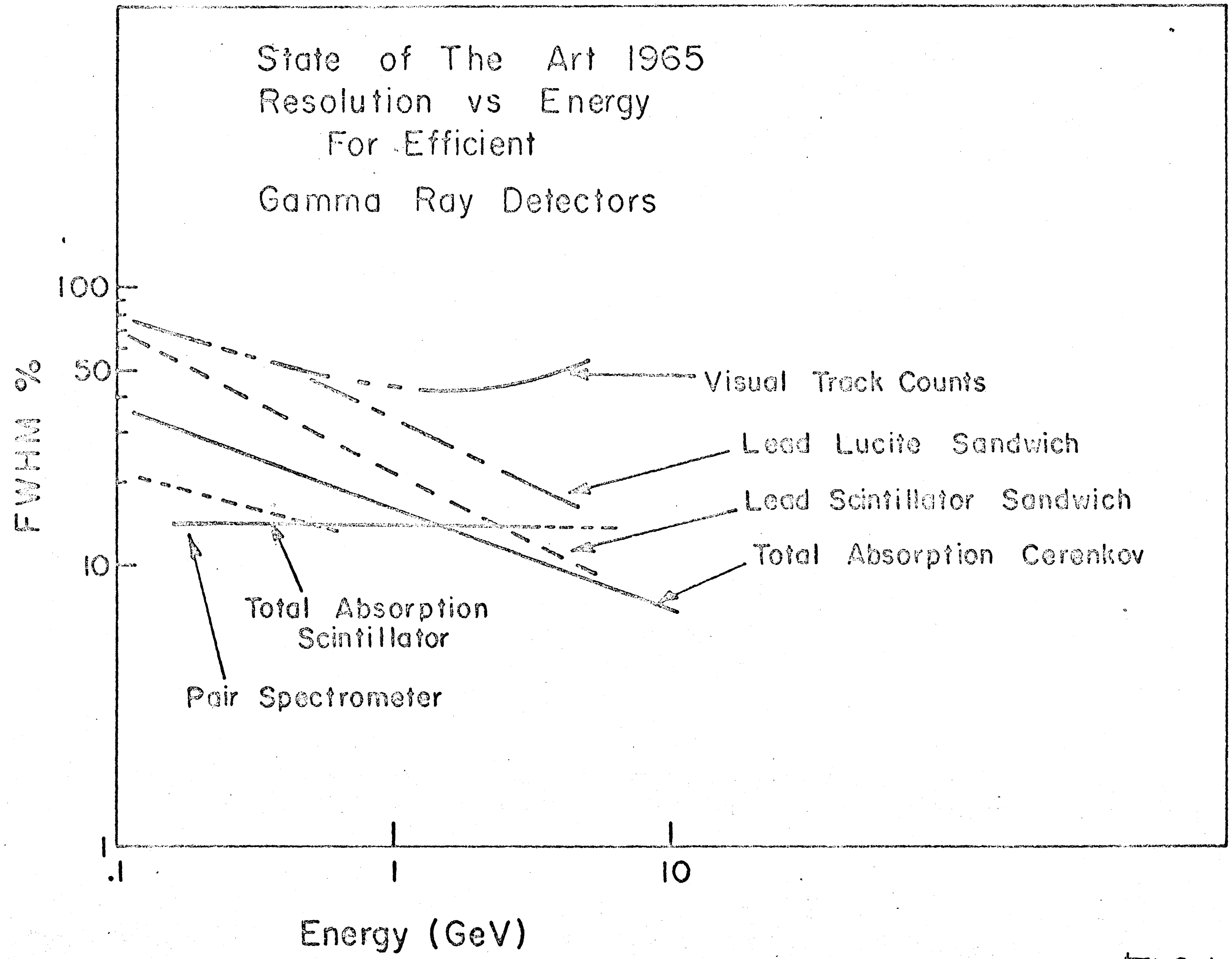
State of The Art 1965
Resolution vs Energy
For Efficient
Gamma Ray Detectors
FWHM %
100
50
10
1
.1
1
10
Energy (GeV)
Visual Track Counts
Lead Lucite Sandwich
Lead Scintillator Sandwich
Total Absorption Cerenkov
Total Absorption Scintillator
Pair Spectrometer

FIG.4.

LEAD SANDWICH DETECTOR

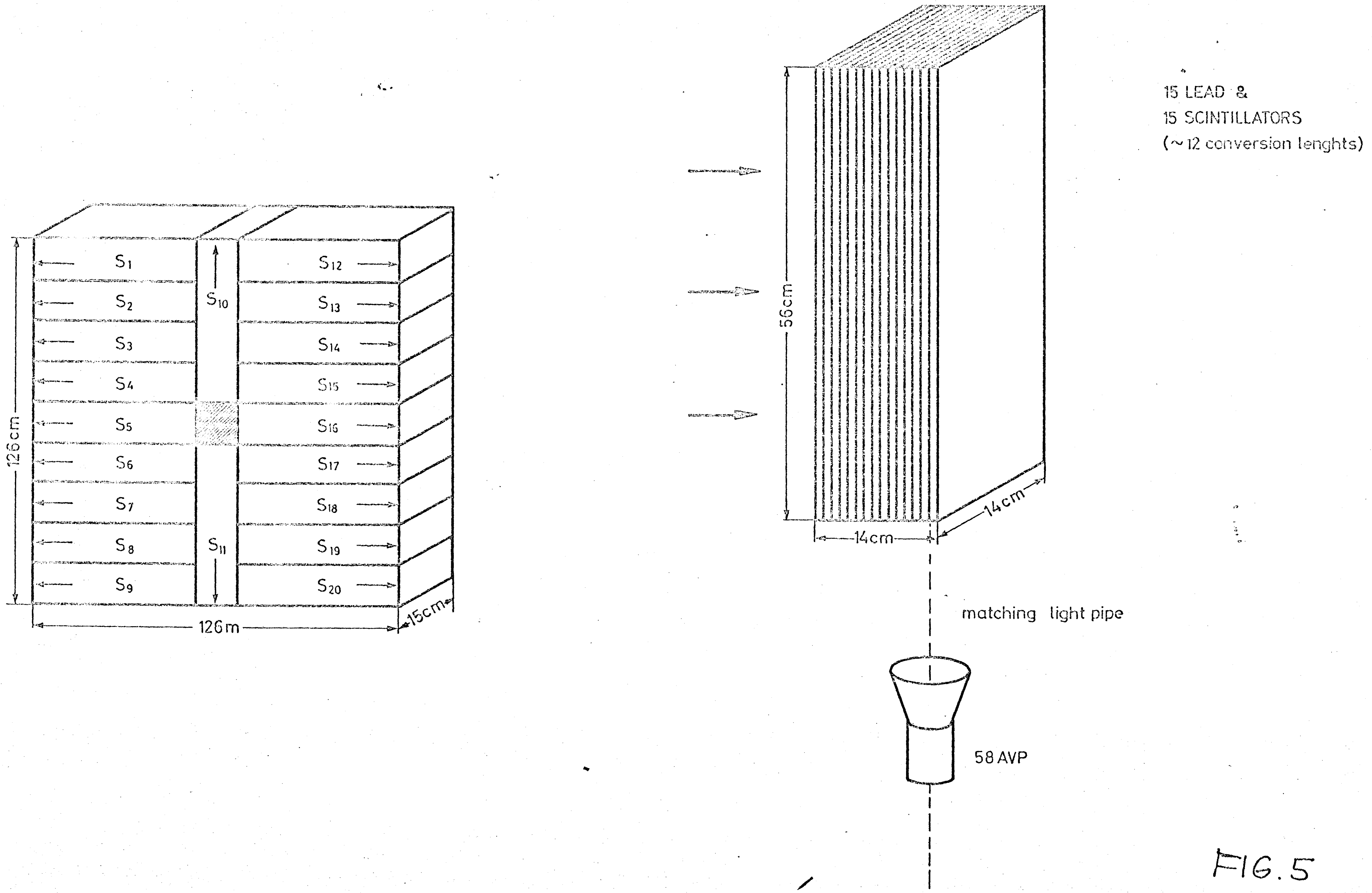

FIG.5

Comparison between lead-scintillator sandwich and lead glas Čerenkov geometrical efficiencies

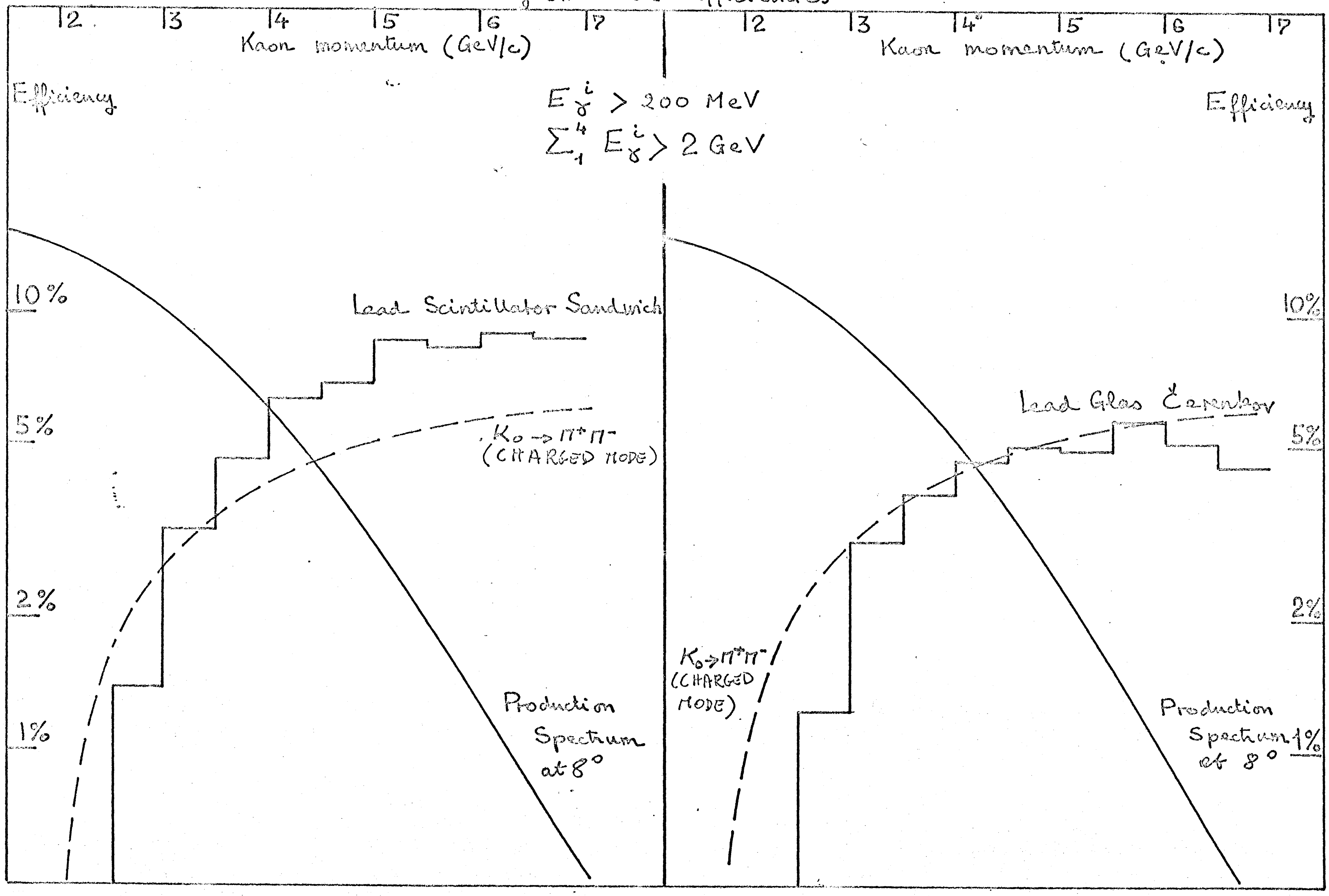

FIG. 6.

Regeneration amplitude ϱ behind a 20 cm Copper Regenerator

$$\psi = K_L\rangle + \varrho K_S\rangle$$

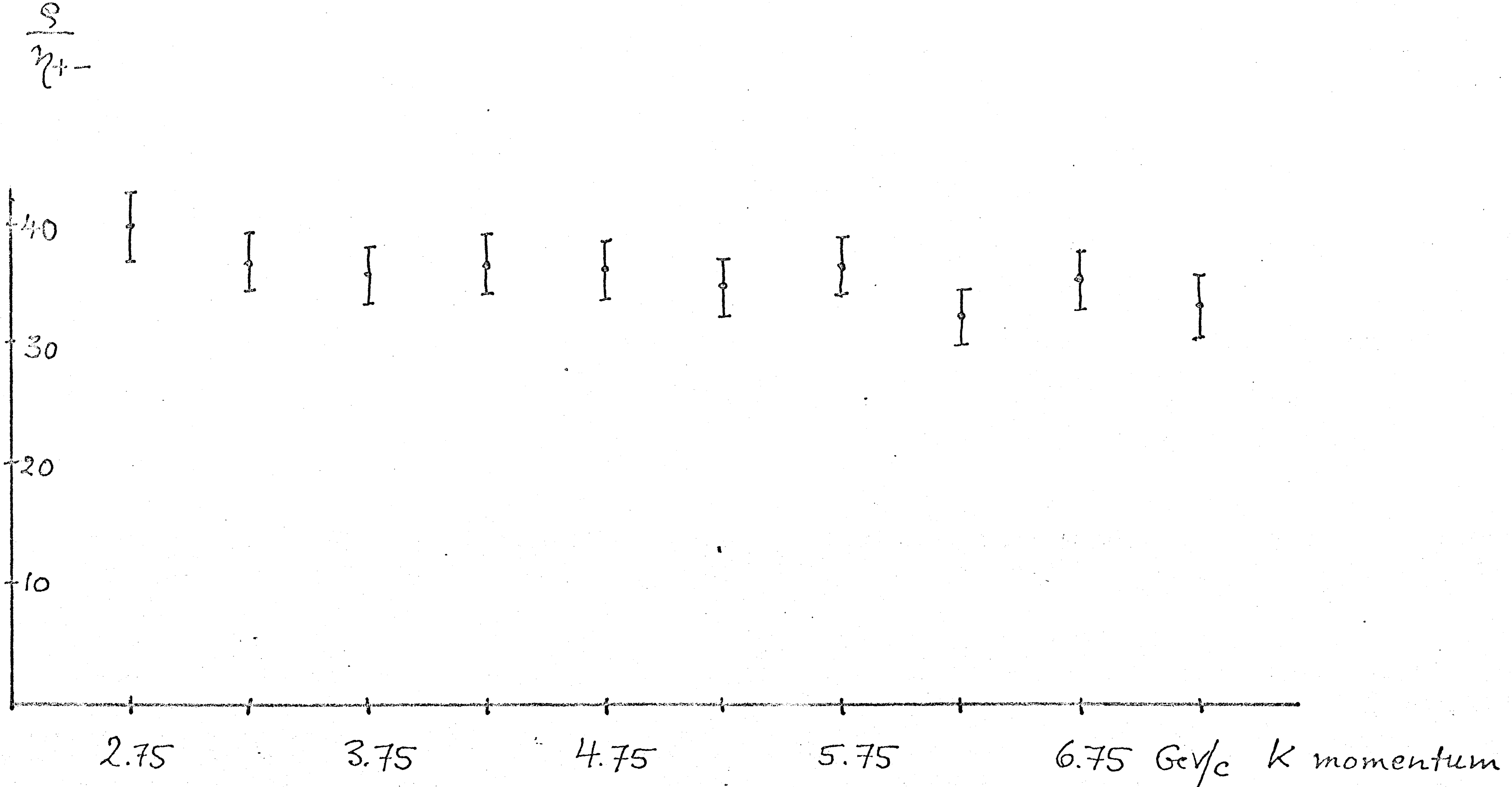

FIG. 7.

Fig 8

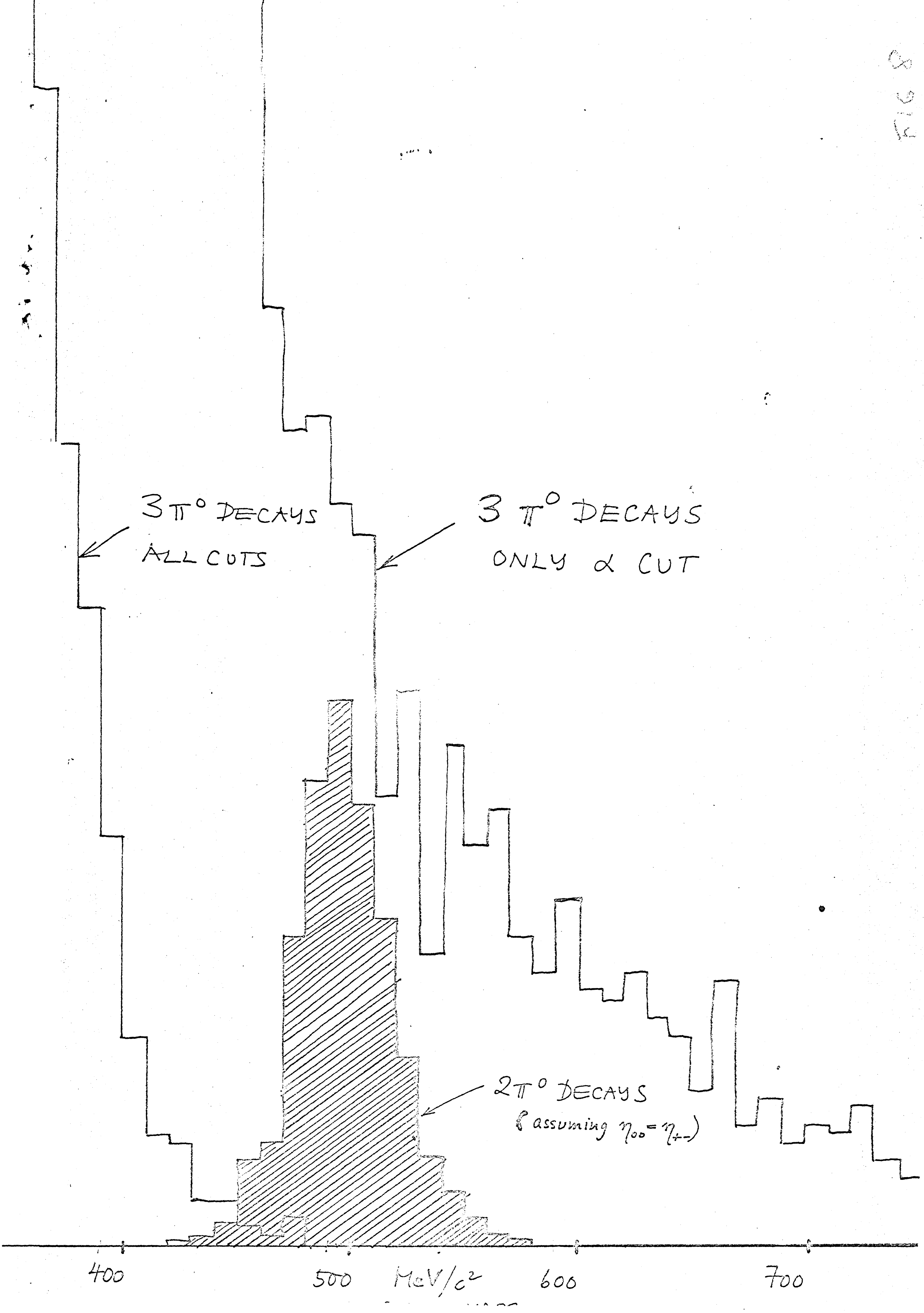
3π° DECAYS
ALL CUTS
3 π° DECAYS
ONLY α CUT
2π° DECAYS
(assuming η₀₀ = η₊₋)
400
500
MeV/c²
600
700